SDEMPED 2003 Symposium on Diagnostics for Electric
Machines, Power Electronics and Drives
Atlanta, GA, USA, 24-26 August 2003

Rotor Cage Fault Detection in Induction Motor using global modulation index on the Instantaneous Power Spectrum

G. Didier[1], *Student Member IEEE*, H. Razik[1], *Senior Member IEEE*, O. Caspary[2] and E. Ternisien[2]
[1] Groupe de Recherches en Electrotechnique et Electronique de Nancy
[2] Centre de Recherche en Automatique de Nancy
Université Henri Poincaré - Nancy 1 - BP 239
F – 54506 Vandœuvre-lès-Nancy, Cedex, France
Tel : +33 3 83 68 41 42 , fax : +33 3 83 68 41 33
e-mail : gaetan.didier@green.uhp-nancy.fr

***Abstract*— Electric motors play a very important role in the safe and efficient running of any industrial plant. Early detection of abnormalities in the motor will help to avoid costly breakdowns. Accordingly, this work presents a technique for the diagnosis of broken rotor bar in induction motor. Stator voltages and currents in an induction motor were measured and employed for computation of the input power of one stator phase. Waveforms of the instantaneous power were subsequently analysed using the Bartlett periodogram. The latter is calculated either with a rectangular window or a Hanning's window. The evaluation of the global modulation index on the instantaneous power spectrum is used for fault detection. Several rotor cage faults of increasing severity were studied with various load effects. We show some experimental results to prove the efficiency of the employed method.**

I. Introduction

The induction motor, especially the asynchronous motor, play an important part in the field of electromechanical energy conversion. It is well-known that the interruption of a manufacturing process due to a mechanical problem induces a serious financial loss for the firm. We know a variety of faults which can occur in induction machines [1] [2], such as rotor faults (broken bar or end ring) or rotor-stator eccentricity. In fact, if faults are undetected, they may lead to potentially catastrophic failures. The consequences of a faulty rotor are excessive vibrations, poor starting performances, torque fluctuation or higher thermal stress. The breaking of rotor bars can be induced by:

- a thermal stress due to thermal overload or unbalance,
- magnetic stresses caused by electromagnetic forces, electromagnetic noise and vibrations,
- a residual stress due to manufacturing problems,
- a dynamic stress arising from shaft torques, centrifugal forces and cyclic stresses,
- environmental stresses caused by contamination and abrasion of rotor material due to chemicals or moisture.

Various techniques have been proposed to detect a rotor fault. One of the well-known approaches for the detection of broken rotor bars in an induction machine is based on the monitoring of the stator currents to detect sidebands around the supply frequency [3] - [10]. Another way to detect a rotor fault is the measurement of torque harmonics, speed or external flux [11].

In this paper, we put forward a broken rotor bars fault detection using the power of the sidebands. It is based on the averaging periodograms. The broken bar detection can be connected to the analysis of the global modulation index. We estimate the global modulation index corresponding to the contribution of all detected sidebands. In order to find the frequency and the amplitude of each sideband to estimate its modulation index and, therefore, we apply a non-parametric power spectrum estimation, called averaging periodograms or Bartlett method. This method is applied on the instantaneous power in induction motor. We show that additional information carried by instantaneous power improves the detection of the sidebands. In fact, the instantaneous power method can be interpreted as a modulation operation in the time domain that translates the spectral components specific to the broken rotor bar to a 0-100 Hz frequency well-bounded. [12] [13].

II. The instantaneous power signature

First of all, we consider an ideal three phase supply voltage. The instantaneous power $p(t)$ of a phase is classically given by:

$$p(t) = v_s(t) i_s(t) \tag{1}$$

where $v_s(t)$ is the instantaneous voltage and $i_s(t)$ is its line current phase. If those two conditions are expected, the supply voltage is sinusoidal and the speed is constant (no ripple), the instantaneous power can be written as follows:

$$v_s(t) = \sqrt{2}V_s\cos(\omega t) \quad (2)$$
$$i_{s0}(t) = \sqrt{2}I_s\cos(\omega t-\varphi) \quad (3)$$
$$p_{s0}(t) = V_sI_s[\cos(2\omega t-\varphi)+\cos\varphi] \quad (4)$$

where φ is the phase angle between the voltage and the current line. The power spectrum of the current has only one fundamental component at the frequency $f_s=\omega/(2\pi)$, while the instantaneous power spectrum has a DC component and its fundamental component at the frequency $2f_s=(2\omega)/(2\pi)$.

When a bar breaks, a rotor asymmetry occurs. The result is the appearance of a backward rotating field at the slip frequency with respect to the forward rotating rotor. This induces in the stator current an additional frequency at $f_{bb_{ts}}=(1-2s)f_s$. This cyclic current variation causes a speed oscillation and a torque pulsation at the twice slip frequency $(2.s.f_s)$. This speed oscillation induces, in the stator winding, an upper component at $f_{bb_{hs}}=(1+2s)f_s$. Briefly, broken rotor bars induce in the stator winding additional components at the frequencies given by :

$$f_{bb}=(1\pm 2ks)f_s \quad (5)$$

where $k=1,2,3,....$

The component at $f_{bb}=(1-2ks)f_s$ does not have the same magnitude as the components at $f_{bb}=(1+2ks)f_s$ because the load inertia intervenes on the latter.

Therefore, the current is modulated [13] - [16] and it can be written:

$$i_s(t) = i_{s0}(t)[1+\sum_h M_h\cos(h\omega_f t)] \quad (6)$$
$$i_s(t) = i_{s0}(t)+\sum_h \frac{\sqrt{2}M_hI_s}{2}[\cos((\omega-h\omega_f)t-\varphi) + \cos((\omega+h\omega_f)t-\varphi)] \quad (7)$$

where $h=1,2,3,....$

As we explained previously, we do not have an amplitude modulation with a perfectly symmetrical modulation law compared to the carrier frequency : the sidebands magnitude on the left and on the right are different but their numbers remain identical. For this reason we have the same index K. The new mathematical equation of the line current gives us:

$$i_s(t) = i_{s0}(t)+\sum_k \frac{\sqrt{2}M_kI_s}{2}\cos((\omega-k\omega_f)t-\varphi) + \sum_k \frac{\sqrt{2}M_k^{'}I_s}{2}\cos((\omega+k\omega_f)t-\varphi) \quad (8)$$

where M_k denotes the modulation index for the left components, $M_k^{'}$ denotes the modulation index for the right components and $f_f=\frac{w_f}{2\pi}=2sf_s$ acts as the modulation frequency. The value of the modulation indexes M_k and $M_k^{'}$ depends on the severity of the abnormality. The expression for the modulated instantaneous power for one phase is obtained by multiplying (2) by (8), is

$$p_s(t) = p_{s0}(t)+\sum_k \frac{M_kV_sI_s}{2}\cos((2\omega-k\omega_f)t-\varphi) + \sum_k \frac{M_k^{'}V_sI_s}{2}\cos((2\omega+k\omega_f)t-\varphi) + \sum_k \frac{V_sI_s}{2}[M_k+M_k^{'}]\cos\varphi\cos(kw_ft) + \sum_k \frac{V_sI_s}{2}[M_k^{'}-M_k]\sin\varphi\sin(kw_ft) \quad (9)$$

In addition to the fundamental frequency and the two sideband components at $f=(2\omega-\omega_f)/(2\pi)$ and $f=(2\omega+\omega_f)/(2\pi)$ for the case of $k=1$, we have, in the instantaneous power spectrum, a spectral peak at the modulation frequency $f_f=\omega_f/(2\pi)$. The latter, referred to as the characteristic component, provides an additional indication of diagnosis information about the motor. Its amplitude depends on phase angle φ and on modulation indexes M_1 and $M_1^{'}$. In our case, this component is used for the calculation of the $2sf_s$ frequency.

III. Broken bar detection based on the global modulation index

In the case of a healthy motor, the equation of the instantaneous power contains an amplitude modulation with one modulation signal around the carrier signal that is the supply power at 100 Hz frequency. In fact, this modulation signal is created by a natural asymmetry of the rotor (eccentricity created by the load for example). If a broken rotor bar occurs, this asymmetry increases and several sidebands appear at the modulation frequencies $2ksf_s$. According to the amplitude modulation theory, if several sinusoidal signals modulate the same carrier wave, the power of this wave does not change while the modulating signals increase the power contained in the sidebands. Since the modulation index is proportional to the amplitude of the modulating signal, different modulation indexes correspond to different modulating signals. The global modulation index M_t is defined so that the power of the sidebands equals the sum of powers of each sideband:

$$\frac{M_t^2P_c}{2}=\sum_k\frac{M_k^2P_c}{2}+\sum_k\frac{M_k^{'2}P_c}{2} \quad (10)$$

where the spectral power P_c of the carrier frequency is $P_c=(V_sI_s)^2$ with the signal $p_s(t)$. The expression of M_t by supposing K_l the number of the sideband components at the left and K_r the number of the sideband components at the right becomes:

$$M_t^2=\sum_{k=1}^{K_l}M_k^2+\sum_{k=1}^{K_r}M_k^{'2} \quad (11)$$

Moreover, for each modulation frequency $2f_s\pm 2ksf_s$, we can deduce its modulation index M_x by dividing its estimated amplitude $A_{s_x}=M_xA_c/2$ by the amplitude of the carrier

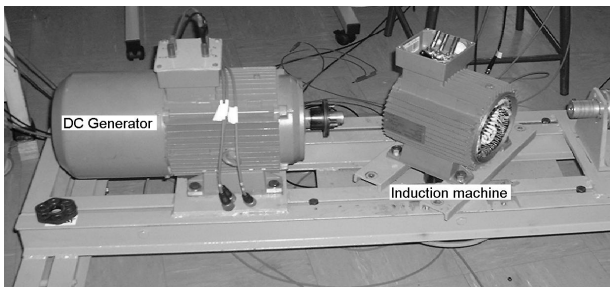

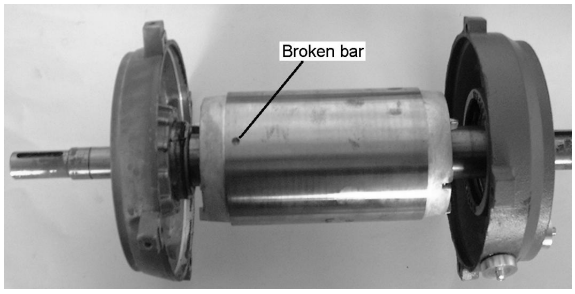

Fig. 1. Test-bed and rotor with one broken bar.

Motor	$2sf_s$ freq	Peaks number N_s	M_{1p}	M_{tp}	M_{1c}	M_{tc}	$2(n_sM_{tp})$	n_sM_{tp}
H-L100	6.89	1	0.0085	0.0128	0.0059	0.0092	**0.0256**	
0.5b-L100	6.95	3	0.0096	0.0149	0.0078	0.0109		0.0447
1b-L100	8.48	3	0.0498	0.0528	0.0361	0.0378		0.1584
H-L50	2.62	1	0.0268	0.0380	0.0154	0.0223	**0.0760**	
0.5b-L50	2.44	2	0.0159	0.0242	0.0062	0.0101		0.0484
1b-L50	2.68	2	0.0258	0.0287	0.0395	0.0484		0.0574

TABLE I

FAULT DETECTION BY GLOBAL MODULATION INDEX WITH A RECTANGULAR WINDOW

Motor	$2sf_s$ freq	Peaks number N_s	M_{1p}	M_{tp}	M_{1c}	M_{tc}	$2(n_sM_{tp})$	n_sM_{tp}
H-L100	6.89	2	0.0032	0.0034	0.0031	0.0033	**0.0136**	
0.5b-L100	6.95	4	0.0055	0.0068	0.0053	0.0063		0.0272
1b-L100	8.48	3	0.0401	0.0422	0.0356	0.0375		0.1266
H-L50	2.62	1	0.0050	0.0053	0.0041	0.0045	**0.0106**	
0.5b-L50	2.44	2	0.0043	0.0055	0.0019	0.0040		0.0110
1b-L50	2.68	2	0.0253	0.0276	0.0264	0.0300		0.0552

TABLE II

FAULT DETECTION BY GLOBAL MODULATION INDEX WITH A HANNING'S WINDOW

frequency $A_c = V_sI_s$:

$$\begin{aligned} \frac{A_{s_x}}{A_c} &= \frac{M_xA_c}{2}\frac{1}{A_c} = \frac{M_x}{2} \\ M_x &= \frac{2A_{s_x}}{A_c} \end{aligned} \tag{12}$$

Thus, the broken bar detection can be connected to the analysis of the global modulation index M_t. We must find the frequency and amplitude of each sideband to estimate their modulation indexes M_k and $M_k^{'}$. Therefore, we apply a non-parametric power spectrum estimation, called averaging periodograms or Bartlett method, instead of the classic periodogram [17]. Indeed, when the record length N increases, the frequency resolution of the periodogram is better but its variance is not reduced. The definition of the periodogram is:

$$\hat{P}_{p_s}(f) = \frac{1}{N}\left|\sum_{m=0}^{N-1} p_s(m)e^{-j2\pi fm}\right|^2 \tag{13}$$

and it can be calculated from a Discrete Fourier Transform (DFT) or a Fast Fourier Transform (FFT). The signal $p_s(m)$ can be windowed if necessary. For the Bartlett periodogram, the data sequence of N samples is divided into L non-overlapping segments of D samples such as $D\,L < N$. The periodograms of each segment are averaged in order to reduce the variance of the Bartlett periodogram as follows [18]:

$$\hat{P}^B_{p_s}(f) = \frac{1}{L}\sum_{i=0}^{L-1}\hat{P}^{(i)}_{p_s}(f) \tag{14}$$

where $\hat{P}^{(i)}_{p_s}(f)$ is the periodogram of the i^{th} segment of the signal $p_s(m)$. Overlapped segments can be used to form the Welch periodogram but it is not necessary in our case because of the high number of samples.

IV. EXPERIMENTAL RESULTS

The test-bed used in the experimental investigation is composed of a three phase induction motor, 50 Hz, 2-poles, 3kW. In order to test the effectiveness of the suggested method, we have several identical rotors which can be exchanged without affecting the electrical and magnetic features. The single squirrel cage has 28 rotor bars (Fig. 1). The voltage and the line current measurements were made at the nominal

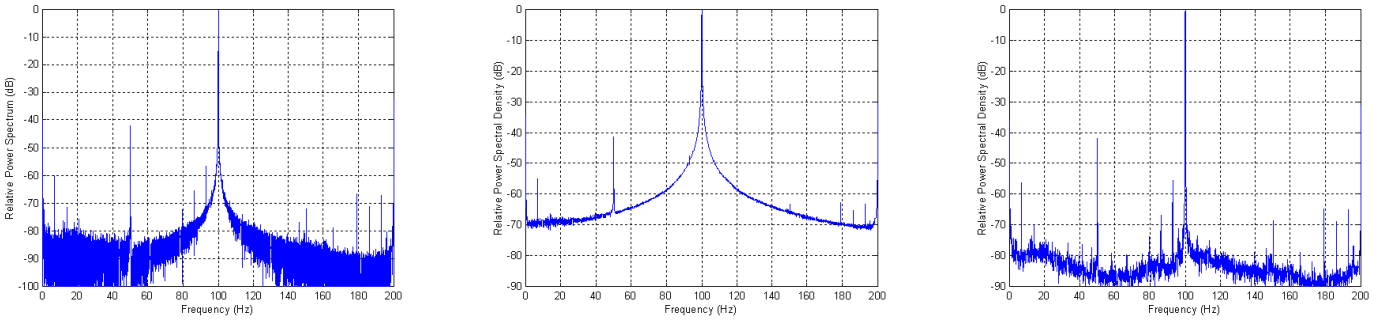

Fig. 2. Classic periodogram of $p_s(t)$ (left), Bartlett periodogram of $p_s(t)$ with Rectangular window (center), Bartlett periodogram of $p_s(t)$ with Hanning's window (right) for the healthy rotor.

rate. For those two variables, the sampling frequency was 2 kHz and each data length was equal to $2^{18} = 262144$ values.

We can see in Fig. 2, which represents the power spectrum of the instantaneous power for the healthy rotor (referred to the 100 Hz fundamental), that the noise level is reduced thanks to the averaging by using the Bartlett periodogram (the data length for the average is equal to 32768 values) . In the case of an allegedly healthy motor with a load (for instance, we note L50 for a load of 50 % and L100 for a load of 100 %), only one spectral component with a low power appears at the frequency 6.89 Hz corresponding to the $2sf_s$ frequency with the use of rectangular window (Fig. 2 (center)). We can see in Fig. 2 (right) that two spectral components appear with the use of Hanning's window, they correspond to $2sf_s$ and $4sf_s$ frequencies.

The obtained spectra are slightly smoothed in the $2kf_s$ band of the additional component of equation 9 but more strongly smoothed around the $100Hz$ due to the contribution of the supply power in the case of the rectangular window. We keep a good estimation of the sideband components power translated from the $0Hz$ by avoiding numerous maxima peaks contained in each one because of a very slight frequency variation of the slip. Consequently, we can consider the detection of maxima peaks in the spectrum. The first frequency that we want to detect is the $2sf_s$ frequency because it corresponds to the sideband with the highest power that is not disrupted by the supply power when we remove the mean of the signal $p_s(m)$. Then, we search all maxima from this first frequency that are at the frequencies $2ksf_s$ in the considered band $[0.2Hz - 35Hz]$ with a greater accuracy (the tolerance is below 1%) and above a threshold defined as the mean of the spectrum. This information gives us the number of components that we must detect around the carrier frequency and the value of s. Thereafter, we calculate the frequencies $2f_s \pm 2ksf_s$ to evaluate their magnitudes. Then, we estimate the modulation index of each modulation frequency in the same way as the equation 12. At the end, with the equation 11, we give the global modulation index on the instantaneous power. The same method is applied to the line current for the determination of the global modulation index around the 50 Hz frequency. A comparison between these two results could be made thereafter.

In the case of 1/2 and 1 broken rotor bar, other spectral components, multiples of the first one, are presented with a greater power (Fig. 3-6). We can note that the influence of the 100 Hz component is reduced in the spectral band near zero and that the lower sidebands detection translated from the zero can be improved. Table I shows the results obtained by the proposed method in the previous section with the use of rectangular window and Table II shows the results obtained with the use of Hanning's window.

N_s represents the peaks number found in the band $[0.2Hz - 35Hz]$. M_{1p} and M_{tp} are respectively the modulation index of the spectral component $2f_s(1-s)$ and the global modulation index detected of the instantaneous power. M_{1c} and M_{tc} represents the modulation index of the spectral component $(1-2s)f_s$ and the global modulation index of the current line. The indexes M_{tp} and M_{tc} give a better estimation than M_{1p} and M_{1c} in the two Tables.

If we look at the global modulation index, the detection of 1/2 and 1 broken rotor bar is possible when there is 100 % load with the rectangular window and the Hanning's window. But when we have 50 % load, only the results obtained with the Hanning's windows allow the broken rotor bar detection. The 1/2 and 1 broken bar with 50 % load are not detected with the modulation index but thanks to the peaks number in the case of the rectangular window. It is not the case with Hanning's window where the global modulation index increases for the two operation (05b-L50 and 1b-L50). We can note that the use of the Hanning's windows is preferable at the rectangular window for the diagnosis of broken rotor bars. Moreover, the results show that the global modulation index M_{tp} increases with more importance than the global modulation index M_{tc} for a same defect. It is more judicious to base the diagnosis of defect on this global modulation index (M_{tp}). Therefore, M_{tp} and the sideband number N_s must be considered inside a criterion that can be of the form: **default if (N_s M_{tp}) measured** $> 2\,(N_s\, M_{tp})$ **of the healthy rotor**. The results of this criterion are written in the last two columns of the Table I and II. The importance of the Hanning's window is clearly shown because with it's use and the criterion quote previously the 1/2 broken bar with a load of 50 % can be detected. If we apply this criterion to the global modulation index M_{tc}, the 1/2 broken bar with a load of 50 % is not

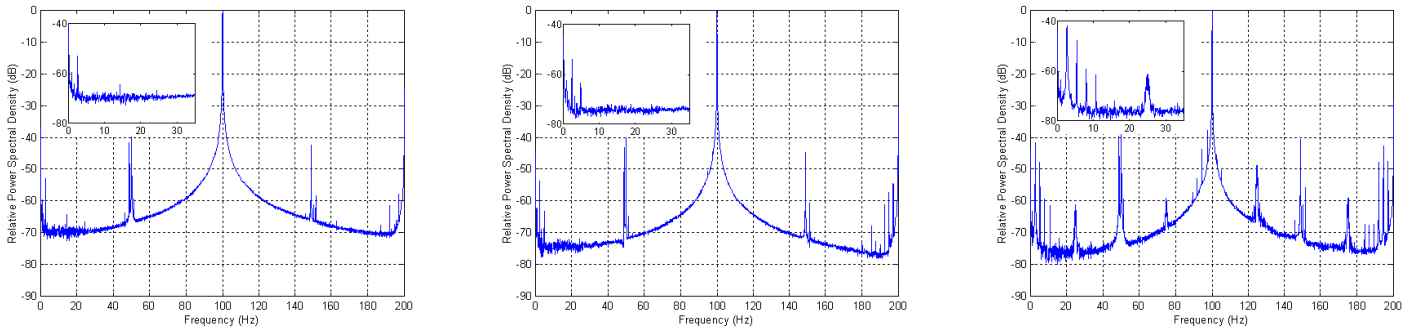

Fig. 3. Bartlett periodogram of $p_s(t)$ with the rectangular window (L50): healthy rotor (left), 1/2 broken bar (center) and one broken bar (right).

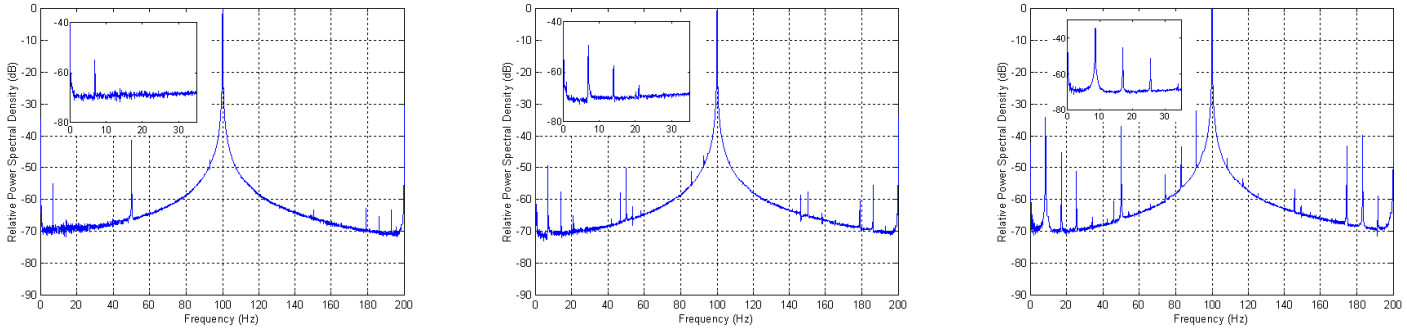

Fig. 4. Bartlett periodogram of $p_s(t)$ with the rectangular window (L100): healthy rotor (left), 1/2 broken bar (center) and one broken bar (right).

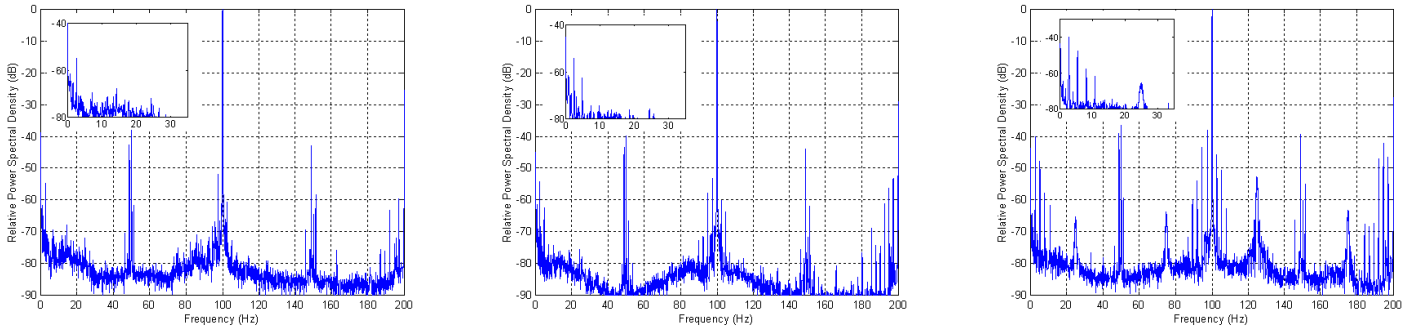

Fig. 5. Bartlett periodogram of $p_s(t)$ with the Hanning's window (L50): healthy rotor (left), 1/2 broken bar (center) and one broken bar (right).

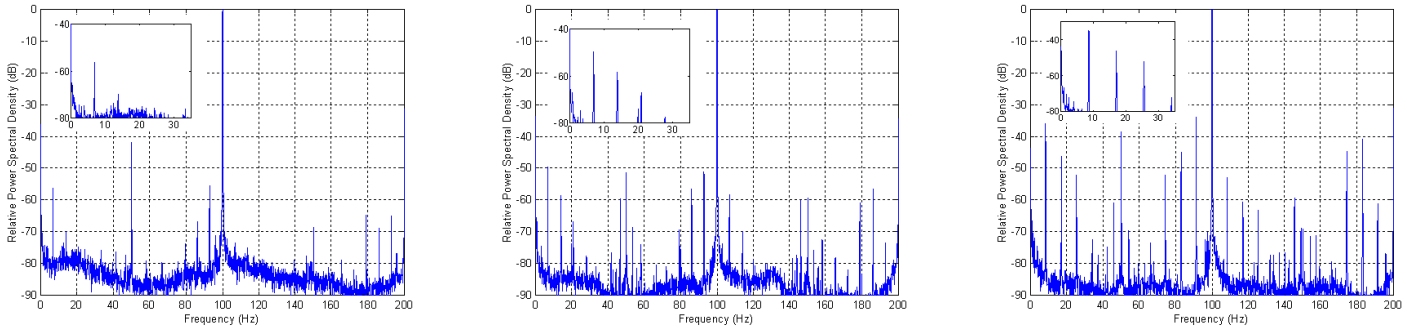

Fig. 6. Bartlett periodogram of $p_s(t)$ with the Hanning's window (L100): healthy rotor (left), 1/2 broken bar (center) and one broken bar (right).

detected. With that last result, we can conclude that the global modulation index applied to the instantaneous power gives more precis results than the global modulation index applied to the line current for the diagnosis of defect in induction motor.

V. Conclusion

The instantaneous power spectrum gives additional components to the modulation frequency $f_f = 2ksf_s$. The latter is the result of the disturbance to the induction motor. The diagnosis based on the global modulation index method applied to the instantaneous power signal provides relevant results for the detection of broken rotor bars. We have demonstrated that a half broken bar with 50 % load can be detected using the criterion which has been developed previously and using a Hanning's window for the computation of the FFT. The experimental results showed us the effectiveness of the technique, even if the motor operates under a low load. The use of the global modulation index on the line current spectrum was carried out. In comparison with the instantaneous power, the line current yields inferior results for the diagnosis of broken rotor bar. We can note that this method can also be used for the diagnosis of mechanical abnormalities in induction motors.

VI. Acknowledgment

The authors wish to express their gratefulness to the Research Ministry and to H. Poincaré University for their financial support in the development of the test-bed.

References

[1] A.H. Bonnet, "Analysis of Rotor Failures in Squirrel Cage Induction Machines," *IEEE Trans. on Industry Applications*, vol. 24, No 6, pp. 1124–1130, November/December 1988.

[2] A.H. Bonnet and G.C. Soukup, "Cause and Analysis of Stator and Rotor Failures in Three-Phase Squirrel-Cage Induction Motors," *IEEE Trans. on Industry Applications*, vol. 28, No 4, pp. 921–937, July/August 1992.

[3] S. Nandi and H.A. Toliyat, "Fault Diagnosis of Electrical Machine - A Review ,"in *IEMDC'99*, pp. 219–221, May 1999.

[4] W.T. Thomson and M. Fenger, "Current Signature Analysis to Detect Induction Motor Faults," *IEEE Trans. On IAS Magazine*, Vol. 7, No. 4, pp. 26–34, July/August 2001.

[5] G.B. Kliman and J. Stein, "Induction motor fault detection via passive current monitoring," in *Proc. ICEM'90*, Vol. 1, pp. 13–17.

[6] G.B. Kliman, J. Stein, R. D. Endicott and R. A. Koegl, "Noninvasive Detection of Broken Rotor Bars in Operating Induction Motor," in *IEEE Transactions on Energy Conversion*, Vol. 3, No. 4, pp. 873–879, December 1998.

[7] R. Fiser and S. Ferkolj, "Detecting Side-band Frequency Components in Stator Current Spectrum on Induction Motor for Diagnosis Purpose," in *Automatika, Journal for Control, Measurement, Electronics, Computing and Communications*, Vol. 40, No. 3-4, pp. 155–160, 1999.

[8] W. Deleroi, "Broken Bar in Squirrel-Cage Rotor of an Induction Motor. Part I: Description by Superimposed Fault-Currents," *Archiv Fur Elektrotechnik*, Vol. 67, pp. 91–99, 1984.

[9] G. Didier and H. Razik and A. Rezzoug, "On the Modelling of Induction Motor Including the First Space Harmonics for Diagnosis Purposes," *International Conference on Electrical Machine ICEM'02* , August 2002.

[10] G. Didier and H. Razik and A. Abed and A. Rezzoug, "On Space Harmonics Model of a Three Phase Squirrel Cage Induction Motor for Diagnosis Purposes," *International Power Electronics and Motion Control Conference EPE-PEMC'02* , Croatia, September 2002.

[11] A. Bellini, F. Filipetti, G. Franceschini, C. Tassoni, G. B. Kliman, "Quantitative Evaluation of Induction Motor Broken Rotor Bars by Means of Electrical Signature Analysis ," in *IEEE Transactions on Industry Applications*, Vol. 37, No 5, pp. 1248–1255, September/October 2002.

[12] R. Maier, "Protection of Squirrel Cage Induction Motor Utilizing Instantaneous Power and Phase Information," *IEEE Transactions on Industry Applications*, Vol. 28, No 2, pp. 376–380, March/April 1992.

[13] M. Benbouzid, "A Review of Induction Motors Signature Analysis as a Medium for Faults Detection," *IEEE Transactions on Industry Electronics*, Vol. 47, No 5, pp. 984–993, October 2000.

[14] S.F. Legowski and A.H.M. Sadrul Ula and A.M. Trzynadlowski, "Instantaneous Power as a medium for the Signature Analysis of Induction Motors," *IEEE Transactions on Industry Electronics*, Vol. 47, No 5, pp. 984–993, October 2000.

[15] M. Drif and N. Benouzza and J.A. Dente, "Rotor Cage Detection in 3-Phase Induction Motors Using Instantaneous Power Spectrum," *Electrimacs'99*, pp. 287–292, 1999.

[16] A.M. Trzynadlowski and E. Ritchie, "Comparative Investigation of Diagnosis Media for Induction Motor: A Case of Rotor Cage Faults," *IEEE Transactions on Industry Electronics*, Vol. 47, No 5, pp. 1092–1099, October 2000.

[17] M.S. Bartlett, "Smoothing Periodograms from Time Series with Continuous Spectra," *Nature*, London, vol. 161, pp. 686-687, May 1948.

[18] S.L. Marple, "Digital Spectral Analysis with Applications," *Prentice-Hall*, New Jersey, 1987.